A deep insight into the Mg–Al–Si nucleosynthesis in massive AGB and SAGB stars

P. Ventura[1]⋆, R.Carini[1,2] and F. D'Antona[1]
[1] *INAF-Osservatorio Astronomico di Roma, Via Frascati 33, Monte Porzio Catone 00040, Italia*
[2] *Dipartimento di Fisica, Università di Roma "La Sapienza", Italy*

ABSTRACT
The stars in globular clusters are known to differ in their surface chemistry: the spectroscopic investigations in the last decades outlined the presence of star–to–star differences in the abundances of the light elements, up to aluminium (and possibly silicon), suggesting that some stars were contaminated by an advanced proton–capture nucleosynthesis. The AGB stars are one of the most promising candidates in producing the pollution of the intra–cluster medium, via the ejection of gas processed by Hot Bottom Burning, from which new stellar generations are formed. This work is focused on the degree of nucleosynthesis involving magnesium, aluminium and silicon that these sources may experience. The key ingredient to determine the degree of magnesium depletion, and the amount of aluminium that can be produced, is the rate of proton capture on ^{25}Mg, forming ^{26}Al; an increase in this cross-section by a factor 2 with respect to the highest value allowed by the NACRE compilation allows to reproduce the extent of the Mg–depletion observed, and is in qualitative agreement with the positive Al–Si correlation observed in a few clusters. The main uncertainties associated with the macro– and micro–physics input, are discussed and commented, and the comparison with recent spectroscopic results for the globular cluster showing some degree of Mg–Al anticorrelation and Al–Si correlation is presented.

Key words: Stars: abundances – Stars: AGB and post-AGB

1 INTRODUCTION

The recent spectroscopic analysis of stars in Globular Clusters (GC) (Carretta et al. 2009a,b) have confirmed the results of the early investigations (Kraft 1994), i.e. the existence of star–to–star chemical differences, that define general abundance patterns, such as the well known O–Na and Mg–Al anticorrelations (Carretta 2006). Such general trends, coupled with the absence of any spread in the heavy elements (Carretta et al. 2009a), and the constant C+N+O (Ivans et al. 1999), indicate that the stars with the most anomalous chemistry are a second generation (SG), formed from gas contaminated by p–capture nucleosynthesis. Among the proposed possible models, one of the most appealing hypothesis is that the intra–cluster medium (ICM) was polluted by the ejecta of intermediate mass stars during their Asymptotic Giant Branch (AGB) phase (Cottrell & Da Costa 1981). The most massive of these objects evolve rapidly compared to the typical age of GCs, and expell gas that was mainly contaminated by Hot Bottom Burning (HBB), with an advanced nucleosynthesis achieved at the bottom of their convective

mantle, and the consequent ejection of matter processed by hydrogen burning (Ventura et al. 2001). The last few years have seen a great improvement in the theoretical description of the evolution properties of Super Asymptotic Giant Branch stars (hereinafter SAGB), i.e. objects whose mass is in the range $6 \lesssim M/M_\odot \lesssim 8$[1], that achieve an off-centre carbon ignition in conditions of partial degeneracy, to end up their evolutionary history as White Dwarfs made up of Oxygen and Neon (see Siess 2006, and references therein). The recent compilation by Siess (2010), in which a complete set of yields from SAGBs of various metallicities are presented, allowed the inclusion of this class of objects together with the AGBs as possible pollutors of the ICM. The terminology "pollution by massive AGBs" can be adopted to indicate the coupled contamination of the ICM by AGB and SAGB stars. The importance of SAGB stars within the context of this scenario is outlined in the paper by D'Ercole

---

⋆ E-mail: paolo.ventura@oa-roma.inaf.it (AVR)

[1] The range of mass involved depends on the assumptions concerning the overshoot from the border of the convective core during the phase of core hydrogen burning. In this work we assume a moderate extra–mixing; if the overshoot had been neglected, the masses of SAGBs would be $8 \lesssim M/M_\odot \lesssim 10$

et al. (2008), where the authors discuss the possibility that these stars provided the gas from which the first–born stars of the second generation formed, a possibility expected to work out only in the most massive clusters.

The yields by AGB stars are uncertain, as they depend critically on the inputs adopted to calculate the evolutionary sequences, not known from first principles. Ventura & D'Antona (2005a) showed that a major role on the predicted physical and chemical properties of these stars is played by the treatment of convection. When a high–efficiency modelling of convection is adopted (i.e. the Full Spectrum of Turbulence developed by Canuto & Mazzitelli 1991) HBB conditions are achieved rather easily for masses exceeding $4M_\odot$; the consequent rapid increase in the luminosity (Blöcker & Schöenberner 1991) favours a large mass loss, thus a smaller number of Thermal Pulses (TPs), and a shorter duration of this evolutionary phase. Under these conditions, the surface chemistry will reflect the HBB equilibria, with little contamination from the Third Dredge–Up (TDU). The different treatment of the convective phenomenology is the main reason for the different results obtained by the various research groups involved in this topic: AGB models in which convection is modelled according to the Mixing Length Theory schematization achieve HBB conditions with more difficulty: Fenner et al. (2004) showed that their yields are not compatible with the chemical patterns observed in GC stars, because they show only a modest trace of HBB contamination.

Ventura & D'Antona (2008, 2009) showed that when convection is modelled with the FST scheme and the mass loss description accounts for the steep increase of $\dot{M}$ with luminosity as soon as HBB is ignited, the yields by massive AGBs are in agreement with the C–N anticorrelation observed in GC stars, and with the depletion of Oxygen detected. The O–Na anticorrelation can also be reproduced, provided that the upper limits for the proton capture reaction by ^{22}Ne nuclei are chosen.

The modelling of SAGBs, for what concerns the HBB phenomenology, is less sensitive to the description of convection, because the core masses are so large that hot bottom burning conditions are easily reached; The yields by these stars are thus expected to show up the imprinting of HBB, although the extent of the nucleosynthesis experienced at the bottom of the convective mantle depends on the mass loss rate, that becomes the main reason of uncertainty (Ventura & D'Antona 2011); although the strength of the pulses is not expected to be strong, the effects of the TDU can also be transported to the surface, provided that a mass loss treatment with a soft dependence on the luminosity is adopted. In comparison with the uncertain chemistry from AGBs, the yields by SAGBs can be reconciled more easily with the patterns observed in GC stars, the only constrain being the use of a mass loss rate steeply increasing with the luminosity (Ventura & D'Antona 2011).

Provided the TDU is weak or made inefficient by the action of strong mass loss rate, the observed C-N and O-Na anticorrelations observed in GCs can be reproduced by the models; the situation is far from being clear for what concerns the observed Mg-Al trend, with the possibile production of silicon.

The aim of the present work is to fill this gap, to understand whether the AGB and SAGB models, that show compatibility with the observed C–N, O–Na anticorrelations, can also reproduce the Mg–Al and Al–Si trends detected in some GCs. To achieve this task we investigate the modality of magnesium burning at the hot bottom of the convective envelope of massive AGBs. We analyze the thermal structure of these layers, to understand whether a significant depletion of the total magnesium, and a simultaneous enhancement in the surface aluminium, can occur, by comparing the burning timescale with the duration of the whole AGB phase. The possibility that some silicon is produced is also addressed. In agreement with previous investigations presented by our group, we also discuss the robustness of these predictions, and their sensitivity to the input–physics adopted.

2 MG-AL NUCLEOSYNTHESIS IN MASSIVE AGBS

A complete analysis of the nucleosynthesis of magnesium and aluminium is given in Arnould et al. (1999). The investigation by Karakas & Lattanzio (2003), though limited to solar or slightly sub–solar metallicity, describes the different sites where the Mg–Al burning is active in AGB stars. The analysis is mainly focused on the nucleosynthesis achieved within the 3α burning shell; the possible action of HBB is considered, but only their $6M_\odot$ model of metallicity Z=0.004 (right–bottom panel of their Fig. 9) shows ^{24}Mg consumption at the bottom of the envelope. The following paper by Karakas et al. (2006) is again focused on the nucleosynthesis in the helium–burning shell, and on the variation in the stellar yields due to the uncertainty in the cross–sections of the α–capture reactions by the magnesium isotopes. A physical context more similar to the present one can be found in Denissenkov & Herwig (2003), that studied the effects of HBB in massive AGBs of low metallicity. Their models outlined the possibility that when the temperature exceeds $\sim 10^8$K the surface ^{24}Mg diminishes, with a consequent increase in the mass fractions of the heavier isotopes. The Mg-Al nucleosynthesis in SAGB stars is studied in details by Siess & Arnould (2008). Finally, the uncertainties of the relevant cross–section of the proton–capture reactions, and how they reflect on the yields from massive AGBs, were discussed in an exhaustive study by Izzard et al. (2007).

The afore mentioned investigations showed that the synthesis of aluminium in AGBs is strictly associated to the activation of proton capture by ^{24}Mg in the innermost regions of the outer convective zone, because this process starts a chain of proton capture reactions, that can ultimely lead to Al–production. The two isotopes ^{25}Mg and ^{26}Mg are also involved in this nucleosynthesis, that will change the overall content of magnesium.

As shown by Denissenkov & Herwig (2003), magnesium burning requires very large temperatures, exceeding $\sim$ 80MK, because the cross-section of the ^{24}Mg(p,γ)^{25}Al reaction, that gives origin to the whole chain, is extremely small at lower temperatures. The rate of ^{24}Mg burning is the most steeply dependent on T, such that in a narrow range of temperatures this process switches from being practically inactive to become the fastest reaction of the whole chain. This is particularly interesting in the case of massive AGB and SAGB stars, because they achieve very large temperatures at the bottom of their convective zone, and are thus
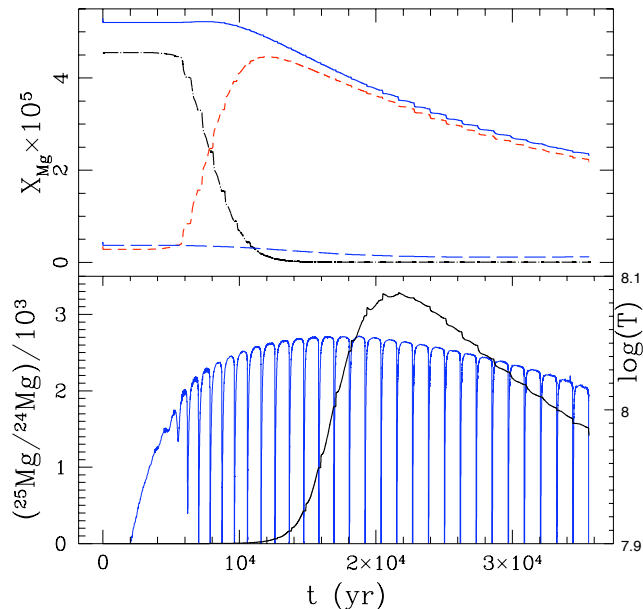
Figure 1. Top panel: variation with time (zeroed at the beginning of the AGB phase) of the surface abundances of the three magnesium isotopes and of the total magnesium in the standard model of mass M=6M$_\odot$. Dot–dashed: ^{24}Mg; short-dashed: ^{25}Mg; Long–dashed: ^{26}Mg; solid: ^{24}Mg+^{25}Mg+^{26}Mg. Bottom panel: variation of the temperature reached at the bottom of the convective envelope (scale on the right) during the TPs, and ratio between the ^{25}Mg and ^{24}Mg abundances.

good candidates to produce gas which is depleted in the total magnesium content and enriched in aluminium.

The top panel of Fig.1 shows the variation with time of the surface content of the three magnesium isotopes and of the total Mg in a model with initial mass 6M$_\odot$, evolved through the whole AGB phase. The behaviour of the temperature at the bottom of the convective mantle and of the ^{25}Mg/^{24}Mg ratio is shown in the bottom panel.

Once the temperature exceeds $\sim 10^8$K, ^{24}Mg burning begins, and proceeds with a time scale of the order of ~ 500 yr, much shorter than the duration of the AGB evolution, $\sim 3 - 4 \times 10^4$ yr. ^{24}Mg has two production channels, i.e. the reactions ^{23}Na(p,γ)^{24}Mg and ^{27}Al(p,α)^{24}Mg, but this latter is always negligible, because ^{27}Al is destroyed preferentially via the alternative channel that leads to the synthesis of silicon. The equilibrium value of ^{24}Mg is therefore $\sim X(^{23}Na)\sigma(^{23}$Na+p$) / \sigma(^{24}$Mg+p$)$, that, for the typical abundances of sodium within the envelope of AGBs, and in the range of temperatures of interest here, is of the order of 10^{-8}. This is much smaller than the initial magnesium content ($X(^{24}Mg)_0 \sim 4 \times 10^{-5}$), so magnesium is destroyed until it reaches such a small equilibrium value after $\sim 10^4$yr (see dotted line in Fig. 1). The exact equilibrium abundance is made uncertain by the scarce knowledge of the abundance of sodium, but this is not particularly relevant for the understanding of the behaviour of the overall magnesium and of aluminium.

The first product of ^{24}Mg burning is ^{25}Mg, which is seen to increase in the early phases of AGB evolution (see the dashed line in the top panel of Fig.1), because the

production channel (proportional to $X(^{24}$Mg$)\sigma(^{24}$Mg+p$)$) largely exceeds the destruction rate (proportional to $X(^{25}$Mg$)\sigma(^{25}$Mg+p$)$). The surface content of ^{25}Mg reaches a maximum when ^{24}Mg is sufficiently depleted, and is later destroyed, with a time scale of the order 3×10^4 yr. This time is comparable to the duration of the whole AGB phase, thus ^{25}Mg never reaches an equilibrium abundance in these thermodynamic conditions; the ^{25}Mg/^{24}Mg ratio (see bottom panel of Fig.1) increases with continuity because ^{24}Mg burning is by far more efficient, and then declines, when the temperature at the bottom of the envelope begins to dimish due to the consumption of the external envelope: this drop in T renders the destruction channel more competitive with respect to the production rate, as a consequence of the different slope with T of the two reactions (see Fig. 3 of Siess & Arnould (2008)).

The behaviour of ^{26}Mg has a scarce impact on these results, because the decay of ^{26}Al, which gives origin to ^{26}Mg, is much slower ($\sim 10^6$ yr) than the ^{26}Al(p,γ)^{27}Si reaction ($\tau \sim 600$ yr), thus favouring ^{26}Mg destrucion, that occurs in a time scale of ~ 5000 yr. ^{26}Mg is thus destroyed during all the AGB phase (long-dashed line in Fig.1), and the overall magnesium content will be given essentially by $X(^{24}$Mg$)+X(^{25}$Mg$)$.

On the basis of these arguments, we conclude that ^{24}Mg is burnt easily at the bottom of the surface mantle of massive AGBs and SAGBs, and the overall depletion of magnesium (hence, the amount of aluminium produced) will be determined by the velocity with which ^{25}Mg, the first product of ^{24}Mg burning, is destroyed. Given the extremely small abundance of ^{26}Mg, once ^{24}Mg destruction occurs the total magnesium will be given by ^{25}Mg, thus the cross section of the reaction ^{25}Mg(p,γ)^{26}Al is the key–quantity in determining the magnesium and aluminium content of the gas ejected by these stars.

The models producing the most extreme chemistries in our context are those with mass at the edge between the AGB and the SAGB regime: we therefore focus on the 6M$_\odot$ models, that are expected to provide the strongest contamination of the ICM (Ventura & D'Antona 2011). Our reference model, which we will refer to as "standard", was calculated with a chemistry typical of intermediate metallicity GCs, i.e. Z=0.001, and [α/Fe]=+0.4; the mixture is taken form Grevesse & Sauval (1998). Convection is addressed within the FST schematization, and mass loss is treated according to the Blöcker (1995) formulation, with the free parameter $\eta_R = 0.02$, in agreement with the calibration given in Ventura et al. (2000). To favour aluminium production, the upper limits for the proton capture reaction by ^{25}Mg nuclei were chosen; this is in agreement with Ventura et al. (1998), where the interested reader may find all the details of the ATON evolution code, used in the present calculations.

Based on the results of the previous section, we focus our analysis of the role played by the choice of the cross–sections by comparing the results obtained when the rate of the reaction ^{25}Mg(p,γ)^{26}Al is doubled with respect to the largest value allowed by the NACRE compilation; this is model 2Mg.

The role of mass loss was investigated by calculating two models with $\eta_R = 0.01$ (Blo01 model), and with a completely different treatment, i.e. the classic recipe by Vas-
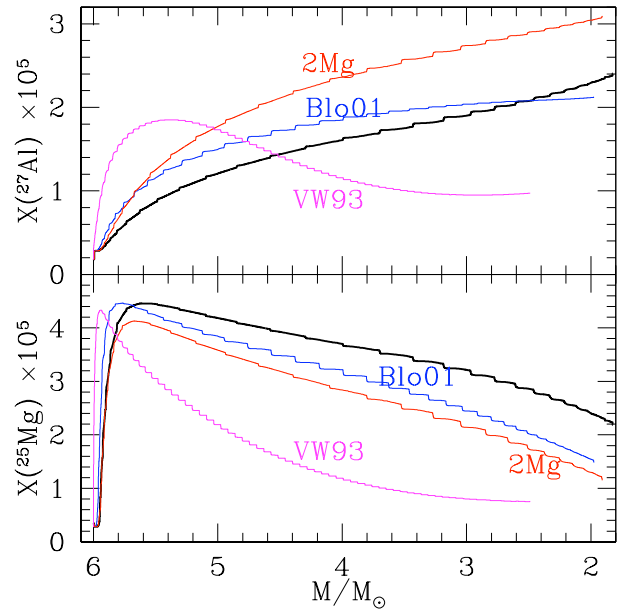
Table 1. Relevant properties of AGB models

Model	τ_{AGB}	$\log(T_{\rm bce}^{\rm max})$	$[^{16}{\rm O}/{\rm Fe}]$	$[{\rm Na}/{\rm Fe}]$	$R({\rm CNO})$	$[{\rm Mg}/{\rm Fe}]$	$[^{27}{\rm Al}/{\rm Fe}]$	$[^{28}{\rm Si}/{\rm Fe}]$	25/24	26/24
standard	3.5×10^4	8.053	-0.40	0.31	0.97	0.27	1.04	0.44	27	1.4
2Mg	3.5×10^4	8.053	-0.40	0.31	0.97	0.13	1.18	0.46	20	1.2
Blo01	5×10^4	8.06	-0.53	0.15	0.94	0.18	1.00	0.49	38	1.6
VW93	9×10^4	8.075	-0.63	0.05	1.65	-0.11	0.83	0.62	117	4
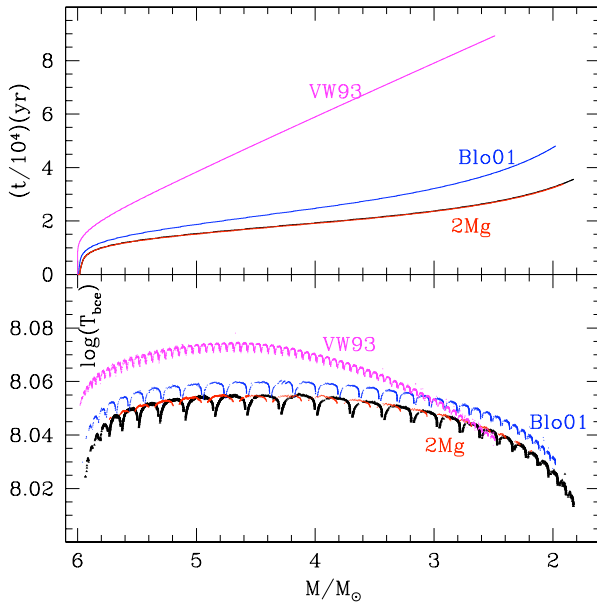
Figure 2. As a function of the total mass of the star we plot the temperature at the bottom of the convective envelope when the H–burning shell is around its maximum efficiency during the TPs (bottom panel) and of the time (starting from the beginning of the AGB phase) of the $6M_\odot$ models (top panel). The acronyms close to the tracks are described in the text —see Table 1.

Figure 3. As a function of the total mass along the tracks, we show the surface abundances of ^{25}Mg and ^{27}Al during the AGB evolution of the four models discussed in the text.

siliadis & Wood (1993) (VW93 model). The description of mass loss has a direct influence on the physical evolution of AGBs, because a higher mass loss favours a more rapid consumption of the whole envelope, with a shorter duration of the AGB phase (Ventura & D'Antona 2005b). Fig.2 shows the variation of the temperature at the bottom of the envelope (bottom panel) , and of the time counted from the beginning of the AGB phase (top), as a function of the total mass (decreasing due to mass loss) during the evolution. The choice of mass (instead of time) as abscissa allows a more direct understanding of the average chemistry of the gas ejected.

The lines corresponding to the models standard and 2Mg cannot be distinguished. Models Blo01 and VW93 evolve more slowly, and, more important, attain higher temperatures at the bottom of their convective zone.

The behaviour of the chemical species of interest is shown in Fig.3. For clarity reasons we only plot the behaviour of ^{25}Mg and ^{27}Al, as we have shown that ^{24}Mg is destroyed rapidly since the early TPs, and eventually the overall magnesium content coincides with the ^{25}Mg left in the envelope. The increase by a factor 2 in the ^{25}Mg(p,γ)^{26}Al cross section favours a 25-30% decrease in the overall magne-

sium. The effect is not directly proportional to the increase in the cross-section used, because ^{25}Mg burning proceeds on time scales $(2-3\times10^4$ yr) comparable to the total duration of this phase ($\sim 4\times10^4$ yr, see Fig.2). The faster depletion of magnesium favours a larger production of aluminium, whose final abundance is increased by $\sim 50\%$ compared to the standard case.

Mass loss modelling also influences magnesium: a slower consumption of the envelope allows a stronger destruction of magnesium, that will survive in smaller quantities within the external mantle. Fig.3 shows that the behaviour of the surface abundance of magnesium is similar in all cases, and the steeper decline of X(^{25}Mg), particularly evident in the VW93 model, is a mere consequence of the smaller mass loss experienced. In the VW93 model the duration of the whole AGB phase becomes so long ($\sim 10^5$ yr, as indicated by the VW93 line in Fig.2) that ^{25}Mg is destroyed until it reaches its final equilibrium abundance, as suggested by the flattening of the dotted–dashed line in Fig.3. This suggests an upper limit to the total magnesium depletion that can be achieved within massive AGBs.

The behaviour of aluminium is even more interesting. The ^{27}Al produced in the envelope increases both in the case when the ^{25}Mg(p,γ)^{26}Al cross section is doubled or with a smaller mass loss still in the Blöcker framework (compare
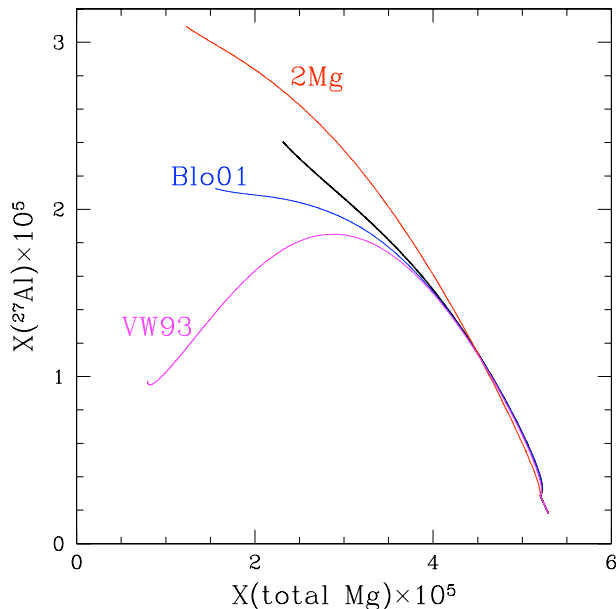
Figure 4. The simultaneous variation of the surface content of magnesium and aluminium in the four models discussed in the text. The lines stop when almost the whole envelope is lost.

the 2Mg and Blo01 lines in Fig.3 with the standard counterpart), but decreases when the VW93 recipe is adopted. The reason for this behaviour is the higher temperature reached at the bottom of the envelope (see also the bottom panel of Fig.2), that favours the activation of ^{27}Al burning with the consequent synthesis of some ^{28}Si. This suggests that there is an upper limit to the amount of aluminium that can be produced within these stars, indipendently of the uncertainties associated to the cross–sections adopted.

The yields of the VW93 model can be compared with those of the same metallicity presented by Siess (2010), based on the same description of the mass–loss mechanism. Such a comparison shows that: a) we achieve a stronger Mg–depletion (δ[Mg/Fe]=−0.5, to be compared to δ[Mg/Fe]=−0.15 by Siess (2010)); b) we produce more Aluminium (δ[Al/Fe]=+0.83, vs δ[Al/Fe]=+0.25). These differences can be understood on the basis of our choice to use the upper limits for the ^{25}Mg(p,γ)^{26}Al reaction, and to the higher magnesium in the α–enhanced mixture used in the present investigation, in comparison with the solar–scaled mixture used by Siess (2010).

The results for the four 6 M$_\odot$ evolutions are given in Table 1. The duration of the AGB evolution (τ_{AGB}), the maximum temperature at the bottom of the convective envelope (T$_{bce}^{max}$), and the O, Na, Mg, Al and Si yields are given. The initial elemental abundances in the star are [X/Fe]=0.4 for O and Mg and [X/Fe]=0 for Na and Si.

Further information include the ratio of the total C+N+O abundances to the initial one (R(CNO)) and the average isotopic ratios ^{25}Mg/^{24}Mg and ^{26}Mg/^{24}Mg in the ejecta. These ratios exceed unity in all cases. The ^{26}Mg/^{24}Mg ratio is less sensitive to the inputs used, because of the scarce impact of ^{26}Mg in the overall magnesium content, and it deviates from unity only in the VW93 case. In agreement with the previous discussions, we find that the

^{25}Mg/^{24}Mg is much more sensitive to the modelling: this ratio decreases when the ^{25}Mg(p,γ)^{26}Al cross–section is increased, whereas it becomes higher when a smaller mass loss rate is used. The isotopic ratios are then ^{25}Mg/^{24}Mg∼20–40. Even larger values, as in other researchers' computations, are found in the VW93 model, where the ratio exceeds 100. This has been considered as a major problem for all the models that attempt to explain the Mg–Al anticorrelation, as the analysis of stars in GCs NGC 6752, M71 and M13 (Yong et al. 2003, 2006) indicate that the (^{25}Mg+^{26}Mg)/^{24}Mg never deviates from unity, even in the most Al–rich objects. We do not discuss this problem any longer, but notice that it can find a simple solution in the framework of a dilution model (e.g. D'Ercole et al. 2008), as it is very easy to alter the high ^{25}Mg abundance by dilution with pristine matter.

The variation of the surface content of aluminium in the four models discussed is shown as a function of the simultaneous change in the total magnesium in Fig. 4. With respect to the standard model, the 2Mg model destroys more magnesium, and produces a larger amount of aluminium: this is a mere consequence of the higher rate for the proton capture reaction by ^{25}Mg nuclei, that moves the equilibrium towards aluminium. The models Blo01 and VW93 also destroy more magnesium, because the lower mass loss rate allows a more advanced nucleosynthesis, both thanks to the longer AGB evolution, and to the larger temperature reached at the bottom of the convective envelope. Unlike the 2Mg case, the total aluminium is decreased compared to the standard model, because the larger temperature favours the ignition of the ^{27}Al(p,γ)^{28}Si, with a partial destruction of the aluminium synthesized. Thus we see that the amount of aluminium that can be produced by the AGB evolution is limited, on the lower boundary, by the HBB temperature and by the evolutionary time spent on the AGB (thus, on the mass loss rate) and, on the higher boundary, by the leakage into silicon, due to proton captures on aluminium.

Comparison of the magnesium yield of the standard track with the value published by Ventura & D'Antona (2011) alerted us to a mistake in the construction of those models, due to an incorrect value of the initial magnesium abundance. We then recomputed all the standard models and provide for clarity a full record of abundances in Table 2. Only the Mg and Al yields differ from the values of Ventura & D'Antona (2011).

The revised magnesium and aluminium yield values of Table 2 for the standard tracks of 6.5, 7, 7.5 and 8M$_\odot$ are then plotted in Figures 6 and 7.

3   COMPARISON WITH DATA

It is now more than 20 years that in GCs star–to–star variations in the surface contents of aluminium and (at a smaller extent) magnesium have been detected. The classic paper by Norris & Da Costa (1995) outlined that the CO–weak stars of ω Cen, NGC 6397, NGC 6752 and M4 were all Al–rich, with enhancements up to more than a factor $\sim$ 10. The question of a possible Mg depletion has been more debated. By examining a large sample of stars in M3 and M13, Cohen & Melendez (2005) claimed a little, if any, Mg depletion in even the most anomalous stars, those showing depleted oxygen and enhanced sodium; this conclusion was at odds

Table 2. Chemistry of the ejecta of SAGB models

Mass($M_\odot$)	$\log(T_{\mathrm{bce}}^{\max})$	$[^{16}$O/Fe]	[Na/Fe]	R(CNO)	[Mg/Fe]	$[^{27}$Al/Fe]	$[^{28}$Si/Fe]	25/24	26/24
6.5M	8.064	-0.24	0.32	0.94	0.34	0.91	0.44	23.5	0.96
7.0M	8.079	-0.15	0.39	0.99	0.36	0.86	0.43	20.7	0.83
7.5M	8.10	0.01	0.67	1.12	0.365	0.65	0.42	8.7	0.39
8.0M	8.16	0.20	1.00	1.19	0.371	0.61	0.40	4.1	0.30

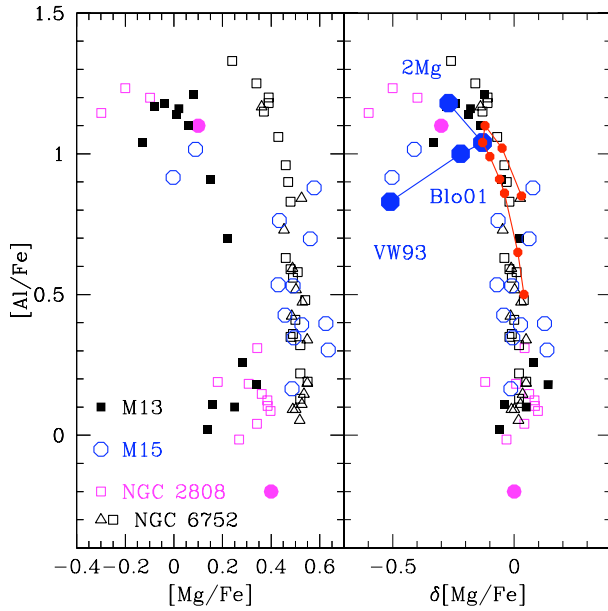**Figure 5.** In the left panel, we show the [Mg/Fe], [Al/Fe] literature data. From Carretta et al. (2009a) we take the data for NGC6752 (open triangles), for M 15 (open circles) and for NGC 2808 (open squares). The extreme Mg abundances for three stars in NGC 2808 are from Carretta et al. (2009b). From Grundahl et al. (2002) we plot data for NGC 6752 (open squares), and from Sneden et al. (2004) the data for M 13 (full squares). The two turnoff stars measured by Bragaglia et al. (2010) in NGC 2808 are plotted as full (magenta) circles. In the right panel we plot the [Al/Fe] as a function of the magnesium variation δ[Mg/Fe] for the different sets of data, and compare it to the theoretical variations expected from AGB and SAGB models. The δ[Mg/Fe] values were obtained by applying to stars belonging to the same cluster a constant shift to [Mg/Fe], so that the stars with the highest magnesium have δ[Mg/Fe]=0. Full large (blue) dots: results from the present investigation. Full small (red) points: AGB and SAGB yields by Ventura & D'Antona (2009) and Table 2. The yields sequence goes from the $8M_\odot$ yield (lowest point) through 7.5, 7, 6.5, 6.3, $6M_\odot$ (the point of the standard evolution), 5.5, 5, 4.5 $M_\odot$.

with the earlier analysis by Sneden et al. (2004). The recent compilation of data from many GCs presented by Carretta et al. (2009a) confirmed in most cases the existence of stars greatly enhanced (~ 1 dex) in their Al content, whereas the Mg–depletion remains within a factor ~ 2; the only exception are three very oxygen poor giants in NGC 2808, that show up a higher Mg reduction (see their Fig.7). Some clusters also exhibit a small Si–enhancement. Yong et al. (2008) find that the nitrogen abundance in the giants of NGC 6752 is positively correlated with silicon, aluminium and sodium,

and anticorrelated with oxygen and sodium. Another interesting result is the recent comparison (Bragaglia et al. 2010) of abundances between two stars belonging to the reddest and to the bluer main sequence of NGC 2808. These two sequences, characterized by a difference in the helium content (Piotto et al. 2007), are expected to represent the original stellar population in the cluster. The measured abundances are [Mg/Fe]=+0.4, [Al/Fe]=−0.2 for the star in the red main sequence, and [Mg/Fe]=+0.1, [Al/Fe]=+1.1 for the bluer object. They are consistent with the hypothesis that stars in the blue main sequence formed from gas processed into the most massive AGBs, and is thus helium rich (D'Antona et al. 2005). If the blue main sequence formed directly from the massive AGB or SAGB ejecta (D'Ercole et al. 2008) it should also be Mg–poor and Al–rich, as found.

In Fig. 5 we select some of the clusters for which Mg and Al data are available. In the left panel we plot the Mg data as they are provided in the references for each set given in the Figure caption. The data for stars with low Al abundances (probably representing the first generation stars) show a large systematic differences, possibly due to intrinsic magnesium differences from cluster to cluster, or to differences in the abundance derivations. In order to compare with models, we then deal with the magnesium variations, shown in the right panel. The standard abundance variations, that is the abundances scaled by 0.4 dex for AGB and SAGB masses from 4.5 to $8M_\odot$ are shown as (red) smaller dots (Ventura & D'Antona 2009, and Table 2). Note that the abundances in the AGB and SAGB ejecta do not vary monotonically with mass, and that the Al (Mg) abundance reaches a maximum (minimum) extent around $6M_\odot$, i.e. for the stars at the edge between the AGB and the SAGB regime. This effect, discussed in detail in Ventura & D'Antona (2011), is due to the high mass loss experienced by the more massive objects, that favours a fast consumption of the whole envelope, before an extreme degree of nucleosynthesis is reached in the external mantle. The evolutions computed in this work are shown as big (blue) dots. We graphically see that the magnesium processing at $6M_\odot$ becomes larger, either by increasing the ^{25}Mg(p,γ)^{26}Al cross section (2Mg dot) or by decreasing the mass loss rate (Blo01 and VW93). The big dots indicate the range of values, expected for the most extreme magnesium depletion and aluminium synthesis, that can be produced within AGBs and SAGBs, for various choices of the mass–loss treatment and cross–sections.

The standard model provides an Al–enhancement in agreement with the Al abundances of the most Al rich stars, while its Mg–depletion, δ[Mg/Fe]=−0.13, appears too small when compared to the most extreme data of M 15, NGC 2808 and M 13. We see that both the increase in the ^{25}Mg(p,γ)^{26}Al cross–section and the decrease in the mass loss rate allows a larger depletion of magnesium, in better

agreement with the observations. The depletion of magnesium in the ejecta of the VW93 model is particularly strong (δ[Mg/Fe]=–0.5), so it would allow to reproduce the smallest observed abundances. However, the yields predicted in this case could hardly reproduce the overall observed picture, because the Al–enhancement would be limited to 0.8 dex, and, more important, no sodium enhancement would occur (see Table 1). Few data would not agree with model 2Mg, and their abundance determinations must be carefully scrutinized before we draw conclusions. Notably, these stars include the three NGC 2808 stars studied by Carretta et al. (2009b), having Mg depleted by 0.5 dex or more, while the blue main sequence star studied by Bragaglia et al. (2010) in the same cluster has a Mg abundance in good agreement with the standard or the 2Mg model.

4 ANY SILICON SYNTHESIS IN GLOBULAR CLUSTERS?

The investigation by Carretta et al. (2009a) indicates a general spread in the silicon abundances detected in the GC stars examined, and a positive correlation between Al and Si. The two lowest panels of their Fig. 10, showing the stars belonging to NGC 2808 and NGC 6752, suggest a positive Al–Si trend, with a slope of about 0.07 (i.e. an increase of 1 dex in the aluminium content is accompanied to a 0.07 dex increase in the measured silicon mass fraction).

The SAGB and AGB silicon variations as a function of the aluminum abundance are plotted in Fig. 6, following the symbols of Fig. 5. Data by Carretta et al. (2009b) for a few clusters are plotted. The stars with the largest Al–enhancement are also expected to be Si–enriched, because part of the aluminium produced is converted into Silicon. The area delimited by the large (blue) dots of the models computed in this work can be considered a measure of the degree of uncertainty of the strongest silicon production, coming form the scarce knowledge of the mass loss rate suffered by these stars, and to the uncertainties associated to the relevant nuclear cross–sections. A larger production of Silicon is obtained when the rate of the p–capture process by ^{25}Mg is increased (2Mg sequence) or when the mass loss rate is assumed to be smaller (Blo01 and VW93 sequences), the difference between the two cases being the opposite behaviour of, as discussed in the previous section. The increase in the rate of the ^{25}Mg(p,γ)^{26}Al reaction favours an increase in the silicon content by δ[Si/Fe]=0.06, which is possibly in better agreement with the data. The silicon synthesis is stronger in the Blo01 and VW93 models; in this latter case an increase δ[Si/Fe]=0.22 is predicted, but these models are in contrast with the sodium abundances. We think that further observational work on the silicon abundances in the clusters showing the strongest chemical anomalies is needed before we can derive stronger constraints on the AGB and SAGB evolution.

5 CONCLUSIONS

We discuss the Mg–Al–Si nucleosynthesis at the bottom of the envelope of massive AGB and SAGB stars, that experience strong HBB during their AGB evolution. The results
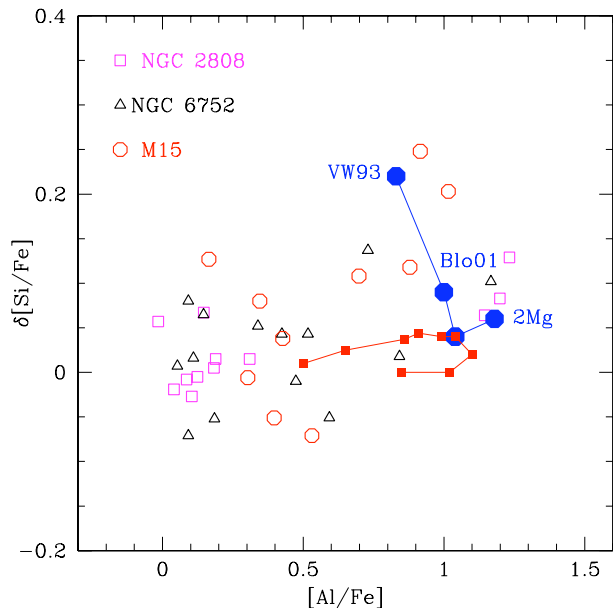

Figure 6. The same as Fig. 5, but referring to the Al–Si plane. The silicon data and yields are normalized in order to show the [Si/Fe] variation.

are compared with data for GC stars, that confirm the existence of a Mg–Al anticorrelation, and show the existence of a positive Al–Si trend. Our goal is to understand whether the same models that allow to reproduce the C–N and O–Na anticorrelations observed, can also account for these patterns involving Mg, Al, and Si. Similarly to the predictions regarding the O–Na trend, we find that when a description of mass loss with a steep dependence on the luminosity is used, the most extreme chemistry, showing the maximum enhancement of aluminium and the strongest depletion of Magnesium, is reached within models of initial mass around $6\mathrm{M}_\odot$, that are at the edge between the AGB and the SAGB regime. SAGB stars, though evolving at higher core masses, loose their mantle very rapidly, before a very advanced nucleosynthesis can occur.

On the nuclear side, we confirm that ^{24}Mg burning is started efficiently in all cases, and proceeds with time–scales so rapid that practically no ^{24}Mg is left within the envelope. Given the small quantities of ^{26}Mg produced, the key–quantity to determine the degree of magnesium depletion, and the amount of aluminium that can be produced, is the rate at which ^{25}Mg nuclei capture protons, to form ^{26}Al; an increase in this cross-section by a factor 2 with respect to the highest value allowed by the NACRE compilation, although not supported by nuclear measurements, allows to reproduce better the extent of the Mg–depletion observed, and is also in better agreement with the slope of the positive correlation between Al and Si detected.

The extent of HBB experienced is also dependent on the treatment of mass loss. Use of a mass loss rate scarcely dependent on the luminosity allows a more advanced nucleosynthesis at the bottom of the convective envelope, that eventually leads to Al–destruction. Although these models can deplete magnesium efficiently, they can hardly agree with the abundance patterns observed, given that the Al-

enhancement is limited to δ[Al/Fe]$=+0.8$ and no sodium production may occur.

REFERENCES

Angulo C., Arnould M., Rayet M., et al., 1999, Nucl.Phys. A, 656, 3

Arnould M., Goriely S., Jorissen A., 1999, A&A, 347, 572

Blöcker T., 1995, A&A, 297, 727

Blöcker T., Schöenberner D., 1991, A&A, 244, L43

Bragaglia A., Carretta E., Gratton R.G., et al., 2010, ApJL, 720, L41

Canuto V.M.C., Mazzitelli I., 1991, ApJ, 370, 295

Carretta E., 2006, AJ, 131, 1766

Carretta E., Bragaglia A., Gratton R., et al., 2009, A&A, 505, 117

Carretta E., Bragaglia A., Gratton R., Lucatello S., 2009, A&A, 505, 139

Cohen J.G., Melendez J., 2005, AJ, 129, 303

Cottrell P. L., Da Costa G. S., 2005, ApJ, 245, L79

D'Antona, F., Bellazzini, M., Caloi, V., Pecci, F. F., Galleti, S., & Rood, R. T. 2005, ApJ, 631, 868

D'Ercole A., Vesperini E., D'Antona, F., Mc Millan S.L.W., Recchi, S., 2008, MNRAS, 391, 825

Denissenkov P., Herwig F., 2003, ApJ, 590,L99

Fenner Y., Campbell, S., Karakas, A.I., Lattanzio, J.C., Gibson, B.K., 2004, MNRAS, 353,789

Grevesse N., Sauval A.J, 1998, SSrv, 85, 161

Grundahl, F., Briley, M., Nissen, P. E., & Feltzing, S. 2002, A&A, 385, L14

Izzard R., Lugaro M., Karakas A.I., Iliadis C., van Raai M., 2007, A&A, 466, 641

Ivans I. I., Sneden, C., Kraft R. P, 1999, AJ, 118, 1273

Karakas A.I., Lattanzio J.C., 2003, PASA, 20, 279

Karakas A. I., Lugaro M. A., Wiescher M., Görres J., Ugalde C., 2006, ApJ, 643, 471

Kraft R. P., 1994, PASP, 106, 553

Norris J.E., Da Costa G.S., 1995, ApJ, 441, L81

Piotto G., Bedin L.R., Andreson J., et al., 2007, ApJ, 661, L53

Siess L., 2006, A&A, 448, 717

Siess L., Arnould M, 2008, A&A, 489, 395

Siess L., 2010, A&A, 512, A10

Sneden C., Kraft R. P., Guhathakurta P., Peterson R. C., Fulbright J. P., 2004, AJ, 127, 2162

Vassiliadis E., Wood P.R., 1993, ApJ, 413, 641

Ventura P., D'Antona F., 2005a, A&A, 341, 279

Ventura P., D'Antona F., 2005b, A&A, 439, 1075

Ventura P., D'Antona F., 2008, A&A, 479, 805

Ventura P., Ventura P., D'Antona F., 2009, A&A, 499, 835

Ventura P., Ventura P., D'Antona F., 2011, MNRAS, 410, 2760

Ventura P., D'Antona F., Mazzitelli I., 2000, A&A, 363, 605

Ventura P., D'Antona F., Mazzitelli I., Gratton, R., 2001, ApJ, 550, L65

Ventura P., Zeppieri A., Mazzitelli I., D'Antona F., 1998, A&A, 334, 953

Vitense E., 1953, Z. Astrophys., 32, 135

Yong D., Grundahl F., Lambert D. L., Nissen P. E., Shetrone M. D., 2003, A&A, 402, 985

Yong D., Aoki W., Lambert D. L., 2006, ApJ, 638, 1018

Yong, D., Grundahl, F., Johnson, J. A., & Asplund, M. 2008, ApJ, 684, 1159